arXiv:hep-ph/9701281v1 13 Jan 1997

Thermodynamics of Constituent Quarks*

H.J. Pirner and M. Wachs

Institut für Theoretische Physik,
Universität Heidelberg

Abstract

We investigate the thermal behavior of quarks and antiquarks interacting via a temperature-dependent linear potential. The quarks are constituent quarks with dynamically generated masses from the background linear σ-model.

1 Introduction

The constituent quark model has been rather successful in meson and baryon spectroscopy [1]. Its main ingredients are massive ($m \simeq 300$ MeV) quark constituents interacting with a potential, which is linear at large distances and coulombic at short distances. A smaller but important role is played by spin-dependent exchange interactions which modify the mass spectra. Recent work on the constituent quark model emphasizes the dynamical nature of the constituent quark mass. A chiral σ-model [2] may be used to generate the quark mass thereby allowing the important coupling of the constituent quark to its pion cloud. By analysing electron scattering on the proton an estimate [3] of the pion cloud of the constituent quark has been obtained. In ref. [4] its effects on baryon spectroscopy have been worked out. The linear σ-model coupled to quarks bears some resemblances to the very popular

---

*Supported by the Bundesministerium für Forschung und Technologie (BMBF) under grant no. 06 HD 742

Nambu-Jona-Lasinio model [6, 7], but it treats the 0^+ and 0^- mesons as fundamental fields. This is an assumption which is true if the system is analysed with a low resolution probe or at moderate temperatures. We would like to argue that up to a temperature $T \approx 250$, MeV i.e. beyond the chiral transition temperature it is still reasonable to separate $(\sigma, \vec{\pi})$ degrees of freedom from the rest of other mesons. Indications in this direction come from lattice simulations [5]. Treating the thermodynamics of the constituent quarks, we allow a deconfinement transition. The thermal gluon fluctuations are modeled to lead to a decreasing string tension with temperature. We neglect all feedback from the quark dynamics to the gluon dynamics. Therefore the decrease of the string tension is given in our model from pure gluon QCD. This way the chiral transition temperature may differ from the temperature where the string tension goes to zero. Actual lattice simulations show a coincidence of the strongly decreasing value of the quark condensate $\langle \bar{q}q \rangle$ and an increasing expectation value of the Wilson loop operator. For dynamical quarks the Polyakov line operator, however, is no longer an order parameter. The problem of double counting the scalar and pseudoscalar degrees of freedom $(\sigma, \vec{\pi})$ as $\bar{q}q$ bound states and as explicit degrees of freedom can be solved by excluding mesons with quantum numbers (${}^1S_0$ and ${}^3P_0$) in the summation over bound $q\bar{q}$ states.

The partition function of the constituent quark model is given as:

$$\mathcal{Z} = \int \mathcal{D}\psi \mathcal{D}\bar{\psi} \mathcal{D}\phi e^{-\int_0^\beta d\tau \int d^3x \mathcal{L}(\psi,\bar{\psi},\phi)} \tag{1}$$

with the Euclidean Lagrangian

$$\begin{aligned} \mathcal{L} &= \bar{\psi}\left(i\gamma\partial - g(\sigma + i\vec{\pi}\vec{\tau}\gamma_5)\right)\psi + (\bar{\psi}\Gamma\psi)_x V(x-y)(\bar{\psi}\Gamma\psi)_y \\ &\quad + \frac{1}{2}\partial_\mu\vec{\phi}\partial_\mu\vec{\phi} + U(\vec{\phi}), \end{aligned} \tag{2}$$

where $U(\vec{\phi}) = -\frac{\mu_0^2}{2}\vec{\phi}\vec{\phi} + \frac{\lambda}{4}(\vec{\phi}\vec{\phi})^2$.

Here $\psi = \begin{pmatrix} u \\ d \end{pmatrix}$ is the spinor of u and d quarks. The meson fields are combined into the four-component vector

$$\vec{\phi} = (\sigma, \vec{\pi}). \tag{3}$$

The parameters of the linear σ-model at $T = 0$ are chosen in such a way that the minimum of the potential $U(\vec{\phi})$ lies at $\langle \sigma_0 \rangle = 0.093$ GeV. The light constituent quarks have a mass of $m = 300$ MeV and the σ mass $m_\sigma = 2m$. Then the couplings are $\mu_0^2 = (0.495 \text{ GeV})^2, \lambda = 28.33, g = 3.23$. These couplings are taken as temperature-independent. The potential V between $q\bar{q}$ in a color singlet state is given by $V_{q\bar{q}}(\vec{x} - \vec{y}) = \kappa|\vec{x} - \vec{y}| - 2\sqrt{\kappa}$ with the string tension $\kappa = \kappa_0 = (447.2\text{MeV})^2$ at zero temperature. The second term takes into account the self energy correction in the constituent quark model [1]. We do not explicitly consider the gluon dynamics, but we consider the string tension as a function of temperature. Lattice simulations for $SU3_{color}$ [9, 10] have determined the critical temperature $T_c = 260$ MeV but not yet the critical behavior, how the string tension decreases with temperature. For large space time dimensions d it is possible to expand around a nontrivial stationary point of the string action. In a $1/d$ -expansion the decrease of the string tension has been calculated as a function of temperature [8]. The effective string tension at finite temperature is

$$\kappa_{eff} = \kappa_0 (1 - (\frac{T}{T_c})^2)^{\frac{1}{2}} \tag{4}$$

with

$$\frac{T_c^2}{\kappa} = \frac{3}{\pi d} + O(d^{-2}). \tag{5}$$

Putting $d = 4$ and neglecting the higher order corrections would give a transition temperature of 220 MeV. We choose the value $T_c = 260$ MeV from lattice simulations. The decrease of κ_{eff} at small temperatures is analogous to the universal Coulomb correction in addition to the linear potential κr.

The above simplified partition function is still rather hard to solve, since the bound states formed at low temperatures will grow in size and overlap with increasing temperature. The resulting problem of a color correlated system of overlapping quark antiquark clusters can probably only be solved with a Monte Carlo calculation [11]. We will limit ourselves in this paper to a simplified analytical calculation, where in the low temperature limit we evaluate the $q\bar{q}$ partition function as a sum over meson bound states. In the high temperature limit we approximate the quarks and antiquarks as a correlated gas with the string potential acting as a perturbation.

The outline of the paper is as follows. In section 2 we calculate the spectrum of a single bound $q\bar{q}$ meson coupled to a heat bath, in section 3 and 4 we compute the partition function of the many-quark and antiquark system in the low and high temperature schemes given above. In section 5 we address the chiral phase transition in mean field theory.

2 Spectrum of a single $q\bar{q}$ bound state coupled to a heat bath

In a first step we neglect the "elementary" mesons $(\sigma, \vec{\pi})$ and take all mesons as bound states of quarks and antiquarks with fixed quark masses. This approximation destroys the nice low temperature behavior of the chiral σ-model, which is governed by the low lying Goldstone pions, but we use this simplification to show our new methods to solve the relativistic bound state problem. This technical development is one of the main new results of this paper. The same method can also be included in more evolved Monte Carlo calculations at finite temperature and finite density. Note that the calculation has to be relativistic since with increasing temperature the mean field mass of the quarks will decrease, so we cannot use the framework of the nonrelativistic constituent model. Instead we propose to treat the partition function of relativistic quarks with the help of auxiliary variables. We start with the example of a single meson composed of a quark and antiquark with total spin

$S = 0$ coupled to a heat bath. The quarks have fixed masses m; then

$$Z_{q\bar{q}} = \mathrm{tr}\exp\left\{-\beta\left(\sqrt{\vec{p}_q^{\,2}+m^2}+\sqrt{\vec{p}_{\bar{q}}^{\,2}+m^2}+V(|\vec{r}_{\bar{q}}-\vec{r}_q|)\right)\right\}. \tag{6}$$

The trick is to rewrite the relativistic Boltzmann factor as follows:

$$\exp(-\beta\sqrt{\vec{p}^{\,2}+m^2}) = \frac{2}{\sqrt{\pi}}\int_0^\infty d\mu\exp\left(-\mu^2-\frac{\beta^2}{4\mu^2}(\vec{p}^{\,2}+m^2)\right). \tag{7}$$

In the appendix we outline the derivation of the full partition function using the same parametrization of the exponential integral as above. Then $Z_{q\bar{q}}$ is given as

$$\begin{aligned} Z_{q\bar{q}} &= \mathrm{tr}\frac{4}{\pi}\int_0^\infty d\mu_1\int_0^\infty d\mu_2 e^{-\tilde{\mathcal{H}}} \\ \tilde{\mathcal{H}} &= \mu_1^2+\mu_2^2+\frac{\beta^2}{4\mu_1^2}(\vec{p}_q^{\,2}+m^2)+\frac{\beta^2}{4\mu_2^2}(\vec{p}_{\bar{q}}^{\,2}+m^2)+\beta V(r). \end{aligned} \tag{8}$$

This allows to separate relative and c.m. motion in the relativistic two-body problem. Of course, we still have a static potential without retardation effects in the interaction. We also do not know how to include relativistic spin-spin and spin-orbit interactions.

The relative and c.m. coordinates are:

$$\begin{aligned} r &= \vec{r}_q-\vec{r}_{\bar{q}} & \vec{p} &= \frac{\mu_2^2\vec{p}_q-\mu_1^2\vec{p}_{\bar{q}}}{\mu_1^2+\mu_2^2} \\ R &= \frac{\mu_1^2\vec{r}_q+\mu_2^2\vec{r}_{\bar{q}}}{\mu_1^2+\mu_2^2} & \vec{P} &= \vec{p}_q+\vec{p}_{\bar{q}}. \end{aligned} \tag{9}$$

With these coordinates the pseudo Hamiltonian $\tilde{\mathcal{H}}$ has the form

$$\begin{aligned} \tilde{\mathcal{H}} &= \mu_1^2+\mu_2^2+\frac{\beta^2m^2}{4}\left(\frac{1}{\mu_1^2}+\frac{1}{\mu_2^2}\right)+\frac{\beta^2}{4}\left[\frac{\vec{P}^2}{\mu_1^2+\mu_2^2}+\frac{\vec{p}^{\,2}}{\mu_1^2\mu_2^2}(\mu_1^2+\mu_2^2)\right] \\ &\quad +\beta V(r). \end{aligned} \tag{10}$$

At this stage it is advantageous to convert to new variables

$$x = \frac{\mu_1^2+\mu_2^2}{\sqrt{2}\beta} \qquad \text{and} \qquad y = \frac{\mu_2^2-\mu_1^2}{\sqrt{2}\beta} \tag{11}$$

which give

$$\begin{aligned}
Z_{q\bar{q}} &= \mathrm{tr}\frac{\sqrt{2}}{\pi}\beta\int_0^\infty dx\int_{-x}^{x} dy\frac{1}{\sqrt{x^2-y^2}}\exp(-\beta h) \\
h &= \sqrt{2}x+\frac{m^2}{2^{3/2}(x-y)}+\frac{m^2}{2^{3/2}(x+y)}+h_{\mathrm{cm}}+h_{\mathrm{rel}}; \\
h_{\mathrm{cm}} &= \frac{\vec{P}^2}{2^{5/2}x} \\
h_{\mathrm{rel}} &= \frac{\vec{p}^2}{m_{\mathrm{red}}}+\kappa_{\mathrm{eff}}r-2\sqrt{\kappa_{\mathrm{eff}}}.
\end{aligned} \tag{12}$$

We see that the separation into a free c.m. Hamiltonian h_{cm} and a Hamiltonian of relative motion h_{rel} has been achieved. The c.m. kinetic energy contains an effective "mass" proportional to x, whereas the energy of relative motion is proportional to the inverse reduced "mass" m_{red}

$$m_{\mathrm{red}} = \sqrt{2}\left(x-\frac{y^2}{x}\right). \tag{13}$$

In the evaluation of the trace we have to sum over all eigenstates of h_{cm} and h_{rel}. The eigenvalues of h_{cm} are plane waves

$$h_{\mathrm{cm}}|\vec{K}\rangle = \frac{\vec{K}^2}{2^{5/2}x}|\vec{K}\rangle. \tag{14}$$

The eigenvalues of h_{rel} can be solved numerically:

$$\begin{aligned}
h_{\mathrm{rel}}\Psi_{n_r,\ell}(r) &= \left(-\frac{\vec{\nabla}^2}{m_{\mathrm{red}}}+\kappa_{\mathrm{eff}}r-2\sqrt{\kappa_{\mathrm{eff}}}\right)\Psi_{n_r,\ell}(r)=\omega_{n_r,\ell}\Psi_{n_r,\ell}(r) \\
\omega_{n_r,\ell} &= \alpha_{n_r,\ell}\sqrt[3]{\frac{\kappa_{\mathrm{eff}}^2}{m_{\mathrm{red}}}}-2\sqrt{\kappa_{\mathrm{eff}}}.
\end{aligned} \tag{15}$$

For the lowest lying states the coefficients $\alpha_{n_r,\ell}$ are as follows: $\alpha_{00} = 2.34$, $\alpha_{01} = 3.36$, $\alpha_{10} = 4.09$ and $\alpha_{02} = 4.25$.

To calculate the equation of state we need the whole spectrum. Instead of numerically calculating the whole spectrum, we take for the higher lying $\bar{q}q$ states the eigenstates of the harmonic oscillator with the ground state adjusted to the exact solution. The high lying states become important at high temperatures, where this approximation is sufficient to get a qualitatively correct picture

$$\omega_{n_r,\ell} \approx (2n_r + \ell + 2.34)\sqrt[3]{\frac{\kappa_{\rm eff}^2}{m_{\rm red}}} - 2\sqrt{\kappa_{\rm eff}}. \tag{16}$$

In principal this approximation is not necessary, but it allows us to use analytical formulas in the following. With the main quantum number $n = 2n_r + \ell$ the degeneracy of harmonic oscillator states is $g(n) = (n+1)(\frac{n}{2}+1)$, the energies are $\omega(n) = (n + 2.34)\sqrt[3]{\frac{\kappa_{\rm eff}^2}{m_{\rm red}}} - 2\sqrt{\kappa_{\rm eff}}$ and

$$Z_{q\bar{q}} = \sum_{\vec{K}} \sum_n g(n) \frac{\sqrt{2}}{\pi} \int_0^\infty dx \int_{-x}^{+x} dy \frac{e^{-\beta\left[\Omega + \frac{\vec{K}^2}{2^{5/2}x}\right]}}{\sqrt{x^2-y^2}} \tag{17}$$

with

$$\Omega = \sqrt{2}x + \frac{m_q^2}{2^{3/2}(x-y)} + \frac{m_{\bar{q}}^2}{2^{3/2}(x+y)} + \omega(n). \tag{18}$$

The c.m. motion can be integrated out giving the final partition function

$$Z_{q\bar{q}} = \frac{2^{5/4}V}{\pi^{(5/2)}} \beta^{-0.5} \sum_n (n+1)\left(\frac{n}{2}+1\right) \int_0^\infty dx x^{1.5} \int_{-x}^{+x} dy \frac{1}{\sqrt{x^2-y^2}} e^{-\beta\Omega}. \tag{19}$$

We project out the bound state meson masses at $T = 0$:

$$M(n_r,\ell)\mid_{T=0} = \lim_{\beta\to\infty}\left(-\frac{1}{\beta}\log Z_{q\bar{q}}\right); \tag{20}$$

In table 1 we give the mass spectrum of relativistic quark antiquark states. The bound states are calculated with fixed constituent masses of 300 MeV for the light quarks and 450 MeV for the strange quarks. The numerical errors are estimated in the following way: The lower values of the masses are obtained from eq. (20) with only the specific state in the partition function. The upper values are gotten

Table 1: Ground state masses M from a relativistic and nonrelativistic calculation for light $q\bar{q}$ and strange quark $s\bar{s}$ states (in brackets) The experimental ρ-meson spectrum is given in addition.

$M(n_r, \ell)$	$1s(0,0)$	$1p(0,1)$	$2s(1,0)$	$2d(0,2)$
relativistic (MeV)	787 ± 7	1205 ± 14	1494 ± 15	1556 ± 15
	(1002 ± 7)	(1391 ± 15)	$(1665 + 15)$	(1724 ± 16)
nonrelativistic (MeV)	900	1422.0	1793.1	1875
	(1064)	(1517)	(1838)	(2190)
exp (MeV)	770	1260	1450	1700
	(1020)	(1285)	(1680)	

by taking into account finite temperature corrections using the free meson partition function

$$Z = \frac{V}{\lambda_T^3} e^{-\beta M} \tag{21}$$

with $\lambda_T = (\frac{2\pi}{M(n_r,\ell)T})^{1/2}$ from eq. (20) for the particular state we are interested in. To compute the upper limits in table 1 we apply eq. (21) with $Z = Z_{q\bar{q}}$. The minimal temperatures are 1.5 MeV for the ground state and 3.0 MeV for the excited states. The obtained spectrum corresponds approximately to the ρ meson spectrum with $\rho(1s)$, $\rho(2s)$, $\rho(2d)$ and the orbital ($\ell = 1$) excitation $a_1(1p)$. The agreement of the theoretical energies with experiment is rather good. Especially the low lying 2s-state is improved by the relativistic Hamiltonian. The splitting between the 2s- and 1s-state of 900 MeV is lowered to the experimentally observed 700 MeV. Note, however, that the spin-dependent interactions are missing. For a constituent quark mass of 450 MeV we obtain the equivalent ϕ-states. Since the physical vector meson states are well described, we can explore the dependence of the meson masses on the choice of quark masses and string tension. Both of these parameters vary with temperature. In fig. 1 we give the dependence of the ground state energy on the constituent mass and on the square root of the string tension. In both cases the ground state energy drops. In the limit of small quark masses the meson mass is of order of $\sqrt{\kappa_0}$. For vanishing string tension the meson mass converges towards twice the quark mass. Here the numerical error of 10 MeV is comparable to the error estimates for the realistic meson masses given in table 1.

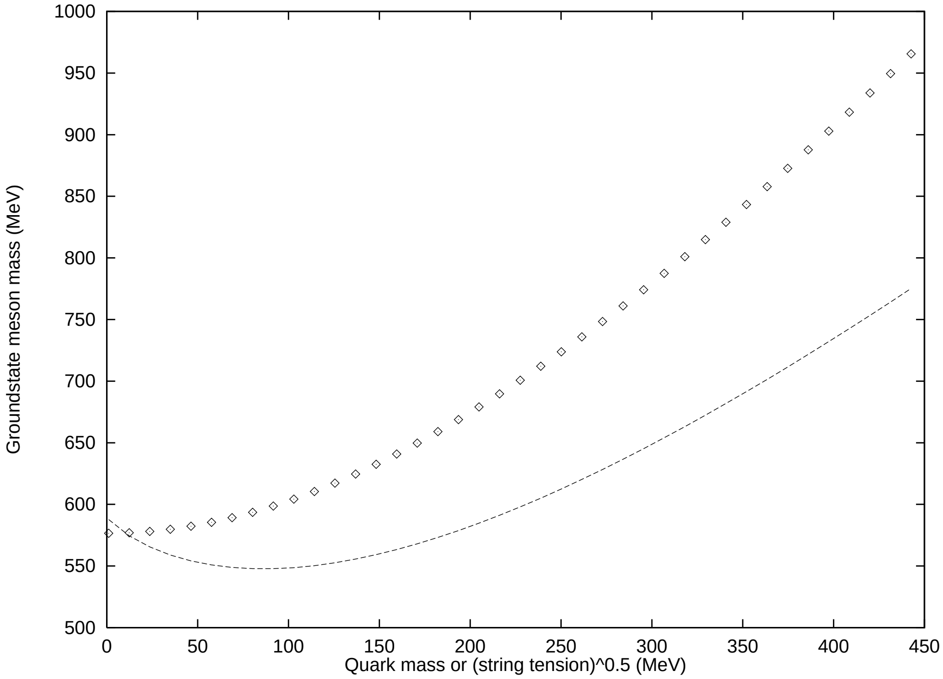

Figure 1: Ground state meson mass as a function of constituent quark mass (squares) and as a function of the square root of the string tension (dashed line).

3 Nonoverlapping $(q\bar{q})$-mesons at low temperature

Now, we address the problem to calculate the partition function Z of a system of N-quarks and N-antiquarks. It can be written as

$$\begin{aligned} Z &= \operatorname{tr}\exp(-\beta\mathcal{H}_N) \\ \mathcal{H}_N &= \sum_{j=1}^{N}\sqrt{\vec{p}_{qi}^{\,2}+m^2}+\sum_{j=1}^{N}\sqrt{\vec{p}_{\bar{q}j}^{\,2}+m^2} \\ &\quad +\frac{1}{2}\sum_{i,j}^{N}V(\vec{r}_{qi}-\vec{r}_{\bar{q}j}). \end{aligned} \tag{22}$$

As before we are limited in our treatment to nonretarded interactions given by the static string tension. In addition we have to sum over all possible arrangements of flux tubes connecting $q\bar{q}$ pairs. To our knowledge this is only possible in a fully dynamical way with a Monte Carlo model, as has been proposed by the Ontario group [11]. In the following we limit ourselves to low temperatures, where the number of mesons is small. Therefore we can safely assume that the individual mesons keep their identity and do not interact. Consequently we have a N-"meson" partition function with the i'th quark always correlated with the i'th antiquark

$$Z = \mathrm{tr} \left(\frac{4}{\pi}\right)^N \prod_{i=1}^{N} \int_0^\infty d\mu_{1,i} \int_0^\infty d\mu_{2,i} \exp -[\mathcal{H}(i)] \tag{23}$$

where for the i'th meson $\mathcal{H}(i)$ is the same Hamiltonian as in the single meson problem

$$\begin{aligned} \mathcal{H}(i) &= \mu_{1,i}^2 + \mu_{2,i}^2 + \frac{\beta^2}{4\mu_{1,i}^2}(\vec{p}_{qi} + m^2) \\ &\quad + \frac{\beta^2}{4\mu_{2,i}^2}(\vec{p}^{\,2}_{\bar{q},i} + m^2) + \beta(\kappa_{\mathrm{eff}} r_i - 2\sqrt{\kappa_{\mathrm{eff}}}). \end{aligned} \tag{24}$$

After the introduction of c.m. and relative coordinates we transform to the variables x_i and y_i as before and get

$$Z = \mathrm{tr} \left(\frac{\sqrt{2}}{\pi}\beta\right)^N \prod_{i=1}^{N} \int_0^\infty dx_i \int_{-x_i}^{+x_i} \frac{dy_i}{\sqrt{x_i^2 - y_i^2}} \exp[-\beta h(i)] \tag{25}$$

with

$$h(i) = \sqrt{2}x_i + \frac{m^2}{2^{3/2}(x_i - y_i)} + \frac{m^2}{2^{3/2}(x_i + y_i)} + \hat{h}_{s_i} + \hat{h}_{\mathrm{rel},i} \tag{26}$$

where

$$\begin{aligned} \hat{h}_{s_i} &= \frac{\vec{P}_i^2}{2^{5/2}x_i}; \\ \hat{h}_{\mathrm{rel},i} &= \frac{\vec{p}_i^{\,2}}{m_{\mathrm{red}}(i)} + \kappa_{\mathrm{eff}} r_i - 2\sqrt{\kappa_{\mathrm{eff}}}; \\ m_{\mathrm{red}}(i) &= \sqrt{2}\left(x_i - \frac{y_i^2}{x_i}\right). \end{aligned} \tag{27}$$

We again use the harmonic oscillator approximation for $\hat{h}_{\mathrm{rel},i}$ given before

$$\begin{aligned}
\hat{h}_{s,i}|\vec{k}_i\rangle &= \frac{\vec{P}_{s_i}^2}{2^{5/2}x_i}|\vec{k}_i\rangle = \frac{\vec{k}_i^2}{2^{5/2}x_i}|\vec{k}_i\rangle \\
\hat{h}_{\mathrm{rel},i}|n_{r,\ell}\rangle &= \left(\frac{\vec{p}_i}{m_{\mathrm{red}}(i)} + \kappa_{\mathrm{eff}} r_i - 2\sqrt{\kappa_{\mathrm{eff}}}\right)|n_{r,\ell}\rangle \\
&= \left(\alpha_{n_r,\ell,i}\sqrt[3]{\frac{\kappa_{\mathrm{eff}}^2}{m_{\mathrm{red}}(i)}} - 2\sqrt{\kappa_{\mathrm{eff}}}\right)|n_{r,\ell}\rangle \qquad (28)
\end{aligned}$$

and

$$\alpha_{n_r,e,i} = (2n_r + \ell + 2.3381). \qquad (29)$$

We consider the integration over the auxiliary parameters x_i and y_i with the measure $\frac{1}{\sqrt{x_i^2-y_i^2}}$ as a summation over intrinsic degrees of freedom of the meson, i.e.

$$\frac{\sqrt{2}}{\pi}\beta\int_0^\infty dx\int_{-x}^{x}\frac{dy}{\sqrt{x^2-y^2}} = \sum_x\sum_y, \qquad (30)$$

then each meson is characterized by the intrinsic parameters $|r\rangle = |k_r, \omega_{n_r}, \ell, x, y\rangle$. The meson many-body wave function is a symmetrized state defined by the occupation numbers of each state $|r\rangle$. The free energy of the mesons has the usual Bose gas form, but now including the summation over the x_i and y_i coordinates

$$\begin{aligned}
F &= \frac{1}{\beta}\sum_{f\bar{f}}\sum_n\sum_k\sum_x\sum_y \ln(1-\exp[-\beta\varepsilon(n,k,x,y)]) \\
&= \sum_{f\bar{f}}\sum_n g(n)\frac{\sqrt{2}}{\pi}\int_0^\infty dx\int_{-x}^{x}\frac{dy}{\sqrt{x^2-y^2}}\frac{V}{(2\pi)^3}\int d^3k\,\ln(1-\exp(-\beta\varepsilon)) \\
&= \sum_{f\bar{f}}\sum_n 2^{5/4}g(n)\frac{\beta^{-1.5}V}{\pi^{5/2}}\int dx x^{3/2}\int\frac{dy}{\sqrt{x^2-y^2}}\sum_{s=1}^{\infty}\frac{1}{s^{5/2}}\exp[-s\beta\varepsilon_r] \qquad (31)
\end{aligned}$$

where

$$\varepsilon(n,k,x,y) = \frac{k^2}{2^{5/2}x} + \varepsilon_r \qquad (32)$$

and

$$\varepsilon_r = \omega_n + \sqrt{2}x + \frac{m^2}{2^{3/2}(x-y)} + \frac{m^2}{2^{3/2}(x+y)}. \qquad (33)$$

We follow the standard way to evaluate the free energy. We first integrate by parts and then rewrite the denominator as a power series before finally integrating the energy of relative motion numerically. To complete the discussion of the meson gas, we also give the expressions for the entropy and energy density

$$\begin{aligned} p &= -F/V; \\ s &= -\frac{1}{V}\left(\frac{\partial F}{\partial T}\right)_V \\ &= \frac{3}{2}\frac{p}{T} + \sum_{f\bar{f}}\sum_n g(n) 2^{1/4}\frac{\beta^{1/2}}{\pi^{5/2}}\int dx x^{3/2}\int\frac{dy}{\sqrt{x^2-y^2}} \\ &\quad \left[\varepsilon_r - \frac{1}{\beta}\frac{\partial\varepsilon_r}{\partial T}\right]\sum_{s=1}^{\infty}\frac{\exp(-\beta s\varepsilon_r)}{s^{3/2}}; \\ u &= Ts - p. \end{aligned} \tag{34}$$

The resulting pressure of the meson gas is shown in fig. 2 for two cases (a) for the ground state mesons only and (b) for the lowest $N = 15$ states. One sees that because of the large meson masses the pressure is rather small up to $T = 150$ MeV. Around this temperature the large number of degrees of freedom for $N = 15$ makes a difference. At a temperature $T = 250$ MeV a Hagedorn transition occurs, when the number of relevant states and consequently the pressure increase tremendously. One sees that the treatment of the system as a gas of noninteracting mesons becomes unrealistic at high temperatures, since the mean distance r_d between mesons becomes smaller than the size of the mesons. The Bose distribution yields the mean particle number $\langle N\rangle$

$$\langle N\rangle = V\sum_{f\bar{f}}\sum_n (2^{5/4}) g(n)\frac{\beta^{-1.5}}{\pi^{5/2}}\int dx x^{3/2}\int dy\frac{1}{\sqrt{x^2-y^2}}\sum_{s=1}^{\infty}\frac{1}{s^{3/2}}\exp[-s\beta\varepsilon_r] \tag{35}$$

and

$$r_d = \left(\frac{1}{\frac{4\pi}{3}\frac{\langle N\rangle}{V}}\right)^{1/3}. \tag{36}$$

The function $r_d(T)$ in fig. 3 is a strongly decreasing function. At $T \simeq 100$ MeV the mean distance between mesons is comparable to the root mean square radius $\sqrt{\langle r^2\rangle}$

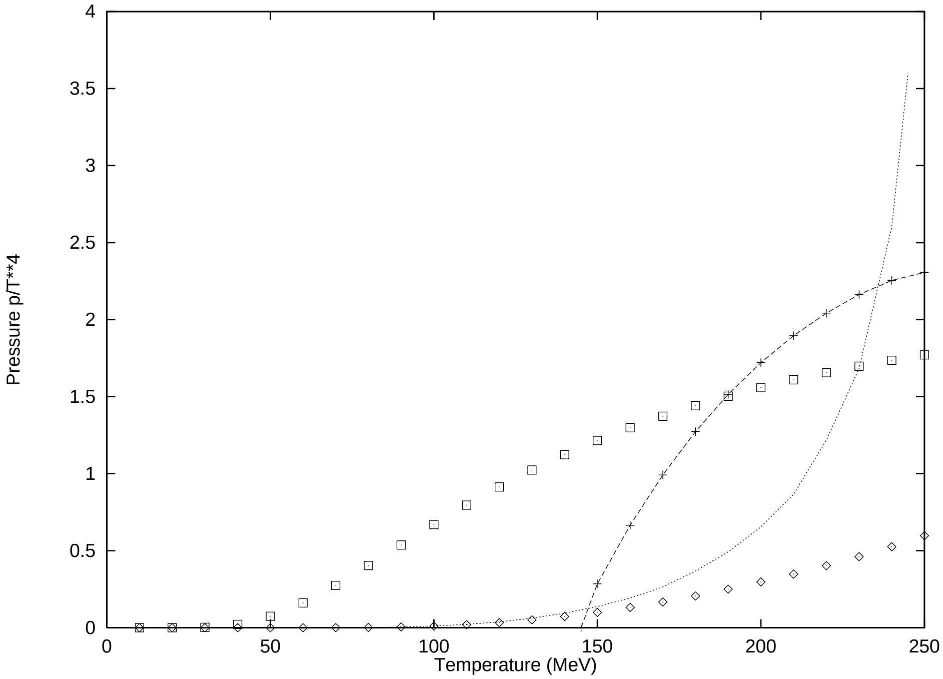

Figure 2: Normalized pressure p/T^4 as a function of temperature T. The lowest pressure is obtained for the confined mesons when only the ground state mesons are considered. A diverging pressure (drawn line) results when mesons with $N = 15$ main quantum numbers are taken into account. For comparison the free $q\bar{q}$ gas pressure (open boxes) and the correlated $q\bar{q}$ pressure (+) are shown.

of the ground state meson

$$\sqrt{\langle r^2 \rangle} = \left(\frac{2.33}{\sqrt[3]{\kappa_{\text{eff}}^2(T)/m \cdot m}} \right)^{1/2} . \tag{37}$$

Around this temperature the approximation of a quasifree meson gas fails, the mesons start to overlap and interact strongly. We also remark that the expression for the entropy leads to a divergent term at $T = T_c = 260$ MeV. This is irrelevant because the assumption of independent mesons already fails at much lower temperatures as discussed above. Clearly, for higher temperatures it becomes more and more inefficient to treat the system as a meson gas and a calculation in terms of quark variables is more advantageous. This does not mean that the strings and their

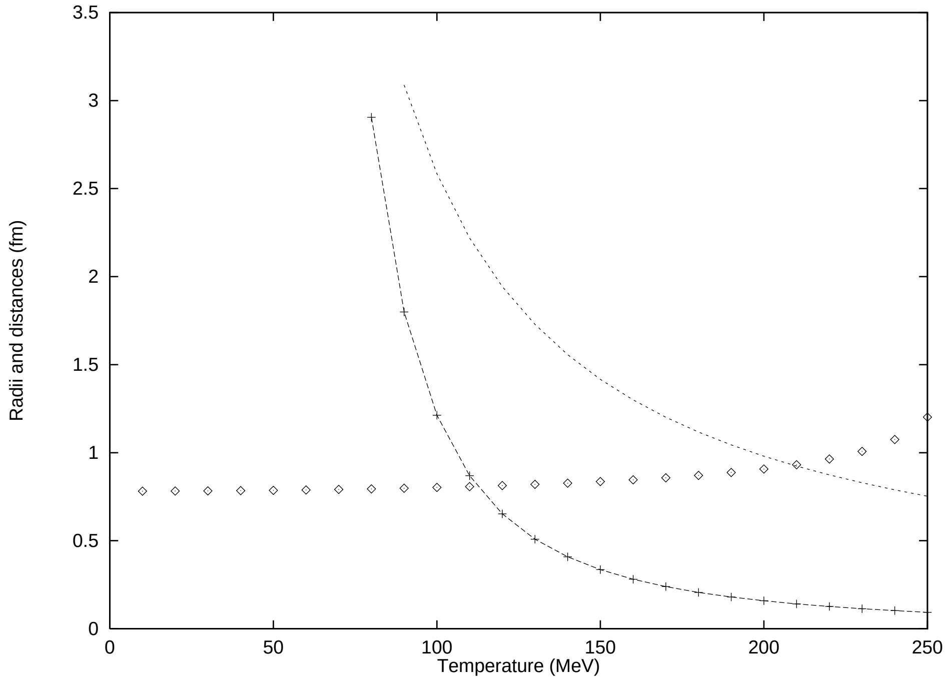

Figure 3: The meson groundstate rms radius (squares) as a function of temperature and the mean distances between mesons r_d (+) and between quarks and antiquarks of opposite color R_{qc} (dashed line).

attractive forces have disappeared. The strings will arrange themselves according to the quark antiquark distributions, instead of extending between fixed pairs of quarks and antiquarks. In fig. 3 one can estimate that near $T = 140$ MeV the mean distance R_{qc} between quarks and antiquarks of opposite color is equal to twice the rms meson radius. After this energy the correlated $q\bar{q}$ system starts to be competitive in energy with the meson system. This will be treated in the next section.

4 Correlated quarks and antiquarks at high temperatures

When the mean distance between quarks and antiquarks becomes smaller than twice the rms radius of the meson state, the mesons will no longer keep their identity, i.e.

the strings will rearrange themselves in configurations with the smallest free energy. An exact calculation probably can only be done with a Monte Carlo simulation. Here we would like to present an estimate using the Hamiltonian given before. The calculation is based on the nearest neighbour saturation of color forces, a concept which has been used in the many quark problem before [12]. In the high temperature limit we consider $\mathcal{H}$ as a sum of noninteracting quark and antiquark energies $\mathcal{H}_\prime$ and a perturbation $\mathcal{H}_\mathcal{I}$

$$\begin{aligned} \mathcal{H} &= \mathcal{H}_0 + \mathcal{H}_I \\ \mathcal{H}_0 &= \sum_q \sqrt{\vec{p}_q^{\,2} + m^2} + \sum_{\bar{q}} \sqrt{\vec{p}_{\bar{q}}^{\,2} + m^2} \end{aligned} \tag{38}$$

$$\mathcal{H}_I = \sum_{\substack{q\bar{q} \\ ff'}} (\kappa_{\text{eff}} |\vec{r}_q - \vec{r}_{\bar{q}}| - 2\sqrt{\kappa_{\text{eff}}}). \tag{39}$$

Here the summation over $r_q, r_{\bar{q}}$ distances is understood under the constraint of a minimal total length of strings. In thermal perturbation theory we first evaluate the free energy related to $\mathcal{H}_0$

$$\begin{aligned} F_0 &= -\frac{1}{\beta} \ln Z_{\bar{q}q} = \sum \ln(1 + e^{-\beta\varepsilon_p}) \\ &= -\frac{24}{\beta} V \int \frac{d^3p}{(2\pi)^3} \ln(1 + e^{-\beta\sqrt{\vec{p}^2 + m^2}}). \end{aligned} \tag{40}$$

The mean number of quarks with a color c equals the mean number of antiquarks with opposite color $\bar{c}$

$$\begin{aligned} \langle N_{qc} \rangle &= \langle N_{\bar{q}\bar{c}} \rangle = 4V \int \frac{d^3p}{(2\pi)^3} \frac{1}{e^{\beta\varepsilon_p} + 1}; \\ &= 4V \sum_{s=1}^{\infty} (-1)^{s+1} \int \frac{d^3p}{(2\pi)^3} e^{-\beta\varepsilon_p s} \\ &= 4V \frac{1}{2\pi^2} m^3 \sum_{s=1}^{\infty} (-1)^{s+1} \left(\frac{2}{\beta^2 s^2 m^2} K_1(\beta s m) + \frac{1}{\beta s m} K_0(\beta s m) \right). \end{aligned} \tag{41}$$

We imagine that each quark is localized in a Wigner Seitz cell of radius R_{qc}. The numerical values of R_{qc} as a function of temperature are shown in fig. 3. The quasilattice of Wigner size cells also of radius R_{qc} for the antiquarks may be shifted relative to the quarks by a distance $|\vec{\ell}| < 2R_{qc}$

$$R_{qc} = \left(\frac{1}{\frac{4\pi}{3} \frac{\langle N_{qc} \rangle}{V}} \right)^{1/3} . \tag{42}$$

Then we can calculate a distribution function for a given quark of color c to find the nearest antiquark with color $\bar{c}$ at a distance r away.

$$\begin{aligned} g(r) \quad = \quad & \frac{1}{\left(\frac{4\pi}{3} R_{qc}\right)^3} \int d\vec{r}_q \; \theta(R_{qc} - |\vec{r}_q|) \\ & \int d\vec{r}_{\bar{q}} \; \theta(R_{qc} - |\vec{\ell} + \vec{r}_q|) \\ & \int d\vec{\ell} \; \theta(2R_{qc} - |\vec{\ell}|)\delta(\vec{r} - (\vec{r}_q - \vec{r}_{\bar{q}})). \end{aligned} \tag{43}$$

In fig. 4 we give the scaled distribution function $g(r/R_{qc})(r/R_{qc})^2$ and compare it to $\theta(1 - r/R_{qc})(r/R_{qc})^2$.

These two curves have approximately the maximum at the same place, but the correlation function extends to larger distances. With this numerically calculated function we calculate the modified free energy in perturbation theory

$$F = F_0 + 3N_{qc}N_{\bar{q}\bar{c}} \langle \mathcal{H}_I \rangle \frac{V_{\text{corr}}}{V} \tag{44}$$

where $\langle \mathcal{H}_I \rangle \cdot V_{\text{corr}} = 4\pi \int g(r/R_{qc}) r^2 dr (\kappa_{\text{eff}} r - 2\sqrt{\kappa_{\text{eff}}})$. The correlation volume $V_{\text{corr}} = 4\pi \cdot R_{qc}^3 \cdot 0.203$ is smaller than the naive volume and the mean $\langle r \rangle = \int r^3 dr g(r/R_{qc}) / \int r^2 dr g(r/R_{qc})$ is unessentially larger than R_{qc}

$$\langle r \rangle = 1.03 R_{qc}. \tag{45}$$

In fig.2 we show the pressure of the correlated quark antiquark gas times $1/T^4$ (with symbols +). It rises rapidly around $T = 150$ MeV and overshoots the uncorrelated pressure at $T \approx 175$ MeV. Near $T = 145$ MeV it already exceeds the still very small pressure of the meson gas. The meson contribution is damped by roughly $e^{-2m/T}$

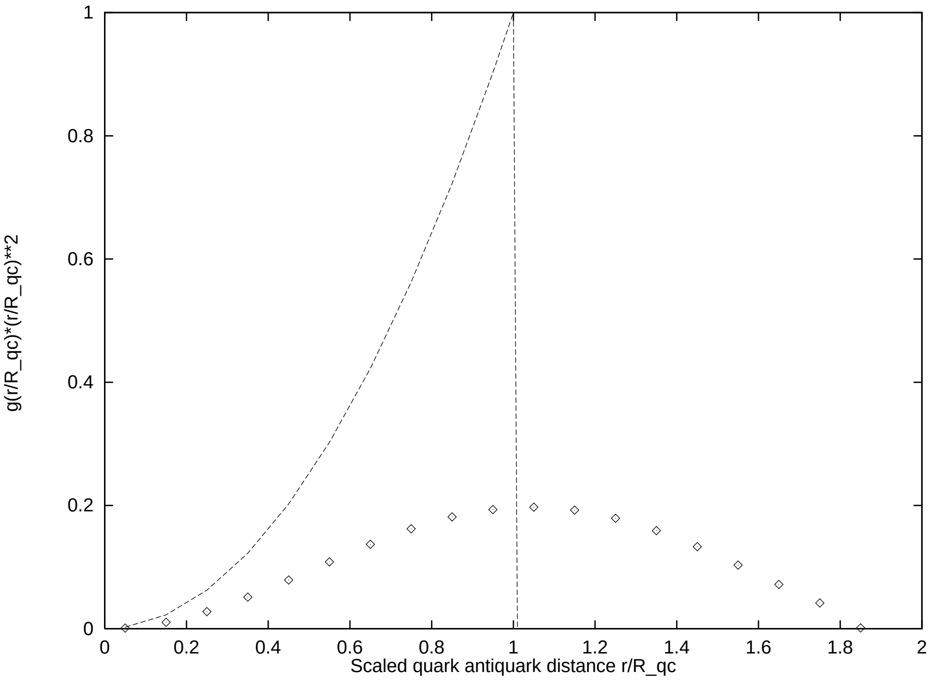

Figure 4: The distribution function $g(r/R_{qc})(r/R_{qc})^2$ (squares) is compared to the uncorrelated theta function multiplied by phase space (line).

compared to the quark excitations which have Boltzmann weights $e^{-m/T}$. The average interaction potential changes sign at $T = 175$ MeV. Of course this value depends critically on the subtraction $2\sqrt{\kappa_{\text{eff}}}$ in the $q\bar{q}$ potential, which gives good agreement with the rho-meson in our model. The inclusion of spin-dependent interactions may modify the potential. The rather simplified calculation presented here conveys the correct message. It is not the "deconfinement" temperature $T_c = 260$ MeV for pure glue theory which determines the phase transition in the presence of quarks, but the lower temperature $T \simeq 145$ MeV where the quarks and antiquarks liberate themselves from the fixed meson configurations. At and above this temperature the quarks and antiquarks are still correlated by strings with a string tension of $\kappa_{\text{eff}}^{1/2}(T = 145 \text{ MeV})$=400 MeV, but these strings change their partners constantly. If this picture is correct, the heavy quarkonia would still experience a long range potential in addition to the modified Coulomb potential due to screening. Also a heavy quark would find additional light antiquarks nearby at no cost in energy. It is in this sense that heavy quarkonia dissolve. The Hagedorn transition of the resonance gas occurring at higher temperature is irrelevant, since it happens outside of the range of credibility of the model. It would actually prefer a system of meson resonances instead of the quark antiquark gas, but at this temperature the resonances are strongly interacting and the independent meson model has lost all its theoretical foundation.

5 Chiral dynamics of constituent quarks

Having set up the formalism for a fixed constituent quark mass we are ready to consider the variation of the constituent quark mass due to the quark condensate. We can use the linear σ-model to generate the quark mass $m = g\langle\sigma\rangle$ where $\langle\sigma\rangle$ is determined from the minimum of the free energies either in the resonance gas phase or in the correlated quark antiquark phase plus the potential energy of the mean σ-field

$$\begin{aligned}\hat{F}_{RG}(\langle\sigma\rangle) &= \sum_{f\bar{f}}\sum_{n} 2^{5/4} g(n)\beta^{-3/2} V \\ &\quad \int_0^\infty dx x^{3/2} \int_{-x}^{+x} dy \frac{1}{\sqrt{x^2-y^2}} \sum_{s=1}^{\infty} \frac{1}{s^{5/2}} e^{-s\beta\varepsilon_r} \\ &\quad + U(\langle\sigma\rangle) \end{aligned} \qquad (46)$$

where

$$\begin{aligned}\varepsilon_r &= (2n_r + \ell + 2.34)\sqrt[3]{\frac{\kappa_{\text{eff}}^2(T)}{\sqrt{2}(x - y^2/x)}} - 2\sqrt{\kappa_{eff(T)}} \\ &\quad + \sqrt{2}x + \frac{(g\langle\sigma\rangle)^2}{2^{3/2}(x-y)} + \frac{(g\langle\sigma\rangle)^2}{2^{3/2}(x+y)}. \end{aligned} \qquad (47)$$

Here one sees how the relativistic bound state calculation takes into account the mean field masses $g\langle\sigma\rangle$ of the quarks via the integration over the auxiliary parameters x and y.

In the high temperature phase of correlated quarks and antiquarks with variable masses the free energy reads

$$\begin{aligned} \hat{F}_{CQ}^{(\langle\sigma\rangle)} &= -\frac{24}{\beta} V \int \frac{d^3\vec{p}}{(2\pi)^3} \ln(1+\exp(-\beta\sqrt{\vec{p}^2+(g\langle\sigma\rangle)^2})) \\ & \quad +3N_{qc}(g\langle\sigma\rangle)N_{\bar{q}\bar{c}}(g\langle\sigma\rangle)\langle\mathcal{H}_I\rangle\frac{V_{\text{corr}}}{V} \end{aligned} \tag{48}$$

where also the interaction energy and the correlation volume depend on the constituent quark mass $m = g\langle\sigma\rangle$, as described in section IV. The mean field quark mass is determined by the condition that the free energies $\hat{F}(\langle\sigma\rangle)$ are minimal, i.e.

$$\begin{aligned} \frac{\partial\hat{F}}{\partial\langle\sigma\rangle}\Big|_{\langle\sigma\rangle=\sigma_0} &= 0; \\ m &= g\sigma_0. \end{aligned} \tag{49}$$

In fig.5 we give the dependence of the constituent quark mass on the temperature for quark matter and resonance matter. In both cases we have a first order phase transition with $T_{\text{chiral}}(CQ) = 147$ MeV, $T_{\text{chiral}}(RG) = 196$ MeV. Until 120 MeV very little change occurs. This is different from calculations of the NJL type with nonconfining interactions. In the line of argumentation given before we do not attribute great significance to the higher chiral phase transition of resonance meson matter, probably a more accurate calculation including the low lying π- and σ-degrees of freedom explicitly would make the two chiral transitions coincide. What is very interesting is the almost coincidence between the deconfinement temperature $T_{\text{dec}} = 143$ MeV, where the resonating meson gas goes over into correlated quark matter and $T_{\text{chiral}}(CQ) = 147$ MeV. This coincidence is surprising given the simplicity of the theoretical calculation. It is dependent on the choice of original constituent quark mass and the behavior of the string tension with temperature. It may indicate that the constituent quark mass is intimately related to the gluon dynamics and the choice of critical behavior of the string tension is perhaps not so far off from reality.

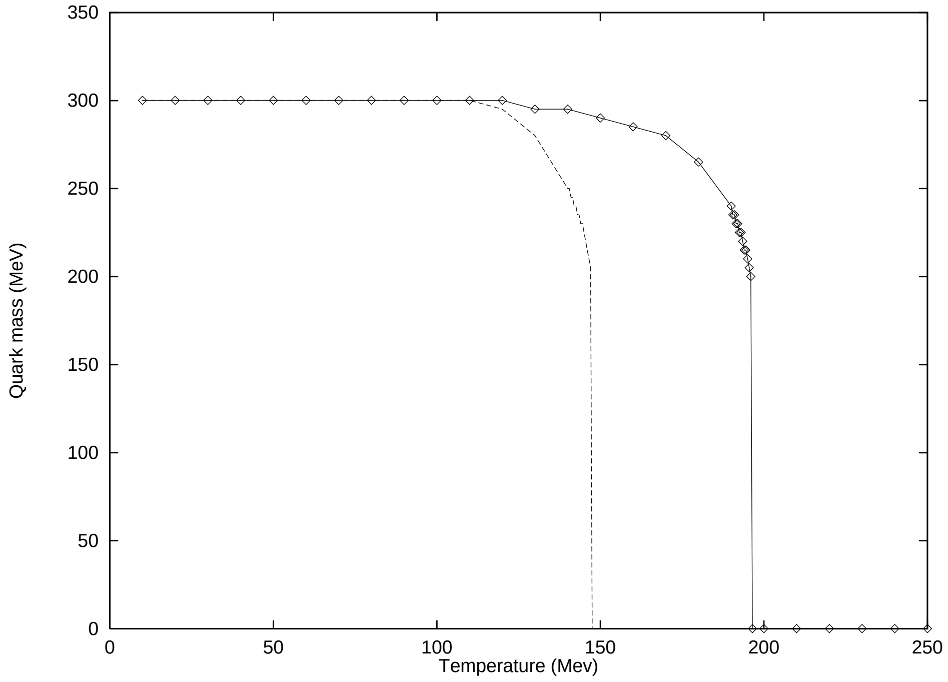

Figure 5: The constituent quark mass as a function of the temperature is shown for the correlated quark antiquark (lines) and for the resonance gas (squares).

6 Conclusions

In the framework of the chiral constituent model we have presented a relativistic calculation of the pressure and the effective quark mass of quarks and antiquarks at finite temperature. At low temperature the constituents are bound in mesons which change their composition only very slowly. Due to the decreasing string tension the quark antiquark bound states have a slightly decreasing mass. In future work we would like to investigate further the ρ meson spectrum as a function of temperature. At temperatures around $T = 120$ MeV the approximation of noninteracting mesons becomes inaccurate and a description in terms of liberated quarks and antiquarks connected by varying string configurations becomes more appropriate. At a temperature $T \approx 145$ MeV both a deconfinement and chiral transition occurs to massless fermions which prefer arranging their string to the nearest antiquark of opposite color nearby. This temperature is distinctly lower than the quark mass transition in the resonance gas occuring at 196 MeV. Important fluctuations of the chiral fields are still missing in the calculation so far. Especially the Goldstone $\vec{\pi}$-fields contribute an important part of the pressure at low temperatures. The addition of these extra degrees of freedom will be done in another paper. In the resonance gas the summation over $q\bar{q}$-bound states should exclude the ${}^1S_0(\vec{\pi})$ and ${}^3P_0(\sigma)$ states. Therefore, for the ground state ${}^3S_1$ and ${}^1S_0$ state the new degeneracy factor becomes $g'(0) = 16 - 3 = 13$ and $g'(1) = 48 - 1 = 47$ for the first excited states, where the 48 states come from the degenerate 4 isospin ${}^3P_0, {}^3P_1, {}^3P_2$ and ${}^1P_1$ channels in the harmonic oscillator model. To evaluate the fermion determinant in the presence of σ and $\vec{\pi}$ fields it is advantageous to use the heat kernel method which has been developed for finite temperatures in ref. [13]. The methods described in this article are not limited to finite temperature. They can as well be applied to finite baryon density, especially to the nuclear problem which has the most promising future. Until now it has resisted any explanation in terms of fundamental quark and string degrees of freedom. Constituent quarks, however, have the correct dynamics in terms of mesonic chiral interactions and confining string dynamics to make the problem accessible.

Appendix

The density matrix for the relativistic two body scalar problem with interaction V neglecting retardation and backward motion has the form:

$$\rho_{q\bar{q}} = \exp[-\beta(\sqrt{\vec{p}_q^{\,2} + m^2} + \sqrt{\vec{p}_{\bar{q}}^{\,2} + m^2} + V(|\vec{r}_{\bar{q}} - \vec{r}_q|))]. \tag{A.1}$$

It has a path integral representation

$$\rho_{q\bar{q}} = \int \mathcal{D}\vec{\nabla}_{\mathrm{II}}\mathcal{D}\vec{\nabla}_{\vec{\mathrm{H}}} \exp[-\int_{,}^{\beta}[\Updownarrow\sqrt{\infty+\dot{\vec{\nabla}}_{\mathrm{II}}^{\,\in}}+\Updownarrow\sqrt{\infty+\dot{\vec{\nabla}}_{\vec{\mathrm{H}}}^{\,\in}}+\mathcal{V}(|\vec{\nabla}_{\vec{\mathrm{H}}}-\vec{\nabla}_{\mathrm{II}}|)]\lceil\tau]. \tag{A.2}$$

This integral can be divided up into a product of integrals over small $\Delta\tau$ intervals which are reformulated with auxiliary fields. The integrals with square roots are transformed into integrals without square roots with the help of the following integral:

$$\exp -\sqrt{a} = \frac{2}{\sqrt{\pi}} \int dx \exp -(x^2 + \frac{a}{4x^2}) \tag{A.3}$$

Eq. (A.3) can be proven by evaluating the integral I and its derivative with respect to a

$$I = \int dx \exp[-(x - \frac{\sqrt{a}}{2x})^2], \tag{A.4}$$

$$\frac{dI}{da} = 0. \tag{A.5}$$

Since the derivative of I with respect to a is zero, the value of I is the norm of the Gaussian integral $I(a=0)$. After a rescaling $x^2 = \mu_1^2\Delta\tau$ and a suitable choice of the measure we obtain the form

$$\exp[-m\sqrt{1+\dot{\vec{r}}_q^{\,2}}\Delta\tau] = \mathcal{N}\int \lceil\mu_\infty \exp[-(\mu_\infty^\in + \frac{\Updownarrow^\in}{\triangle\mu_\infty^\in}(\dot{\vec{\nabla}}_{\mathrm{II}}^{\,\in} + \infty))\cdot\tau] \tag{A.6}$$

Multiplying the individual time slices with each other one generates the full density matrix

$$\begin{aligned}\rho_{q\bar{q}} \;&=\; \mathcal{N}' \int \mathcal{D}\vec{\nabla}_{\mathrm{II}}\mathcal{D}\vec{\nabla}_{\vec{\mathrm{H}}}\mathcal{D}\mu_\infty\mathcal{D}\mu_\in \qquad\qquad (A.7)\\ &\exp[-\int_0^\beta[\mu_1^2+\mu_2^2+\frac{m^2}{4\mu_1^2}(1+\dot{\vec{r}}_q^{\,2})+\frac{m^2}{4\mu_2^2}(1+\dot{\vec{r}}_{\bar{q}}^{\,2})+V(|\vec{r}_{\bar{q}}-\vec{r}_q|)]d\tau.\end{aligned}$$

In general the auxiliary fields are functions of τ. We propose as an approximation to keep only auxiliary fields in the functional integral which are independent of time.

Then the path integral over $\mathcal{D}\vec{\nabla}_{\amalg}\mathcal{D}\vec{\nabla}_{\bar{\amalg}}$ can be executed by solving the corresponding two-body Schroedinger equation

$$[-\frac{\vec{\nabla}_q^2}{4\mu_1^2} - \frac{\vec{\nabla}_{\bar{q}}^2}{4\mu_2^2} + V(|\vec{r}_{\bar{q}} - \vec{r}_q|)]\Psi(\vec{r}_q, \vec{r}_{\bar{q}}) = E(\mu_1, \mu_2)\Psi(\vec{r}_q, \vec{r}_{\bar{q}}). \tag{A.8}$$

The final integration over the auxiliary fields becomes a two-dimensional integration

$$\rho_{q\bar{q}} = \mathcal{N}' \int \lceil\mu_\infty \lceil\mu_\in \exp[-\int_/^\beta [\mu_\infty^\in + \mu_\in^\in + \frac{\Updownarrow^\in}{\triangle\mu_\infty^\in} + \frac{\Updownarrow^\in}{\triangle\mu_\in^\in} + \mathcal{E}(\mu_\infty, \mu_\in)]\lceil\tau]. \tag{A.9}$$

Finally the partition function can be written in the form of eq. 8 of section 1 by the substitution $\beta\mu_1^2 \to \mu_1^2$ and $\beta\mu_2^2 \to \mu_2^2$. The normalization factor in front of the integral in eq. 8 is adjusted to reproduce the free partition function without potential.

Acknowledgements

We would like to thank B. J. Schaefer for a careful reading of the manuscript and our colleagues in the Rhein-Main-Neckar group on Relativistic Heavy Ion Physics for their critical and helpful comments.

References

[1] W. Lucha, F.F. Schoebel, and D. Gromes, Phys. Rep. **200**, 127-240 (1991).

[2] A. Goksch, Phys. Rev. Lett. **67**, 1701 (1991).

[3] S. Baumgaertner, H.J. Pirner, K. Koenigsmann, and B. Povh, Z. Phys. **A353**, 397 (1996).

[4] L.Y. Glozmann and D. O. Riska, Phys. Rep. **268**, 263-303 (1996).

[5] K.D. Born, S. Gupta, A. Irbaeck, F. Karsch, E. Laermann, B. Petersson and H. Satz, Phys. Rev. Lett. **67**, 302 (1991)

[6] T. Hatsuda and T. Kunihiro, Phys. Rep. **247**, 221- 367 (1994).

[7] S. Klevansky, Rev. Mod. Phys. **64**, 649-708 (1992).

[8] R.D. Pisarski and O. Alvarez, Phys. Rev. **D26**, 3735 (1982)

[9] F. Karsch, “The Phase Transition to the Quark Gluon Plasma”, Int. Conference on Ultra Rel. Heavy Ion Collisions, Monterey (1995).

[10] G. Boyd, J. Engels, F. Karsch, E. Laermann, C. Legeland, M. Luetgemeier, and B. Petersson, BVVi-Tp 96/04, Bielefeld preprint.

[11] P.J.S. Watson, Nucl. Phys. **A494**, 543 (1989).

[12] G. Roepke, D. Blaschke and H. Schulz Phys. Rev.**D34**, 3499 (1986)

[13] B.J. Schaefer, Dissertation Heidelberg (1996).